Square Pyramidal Clusters in La_3In_5 and Y_3In_5. La_3In_5 as a Metallic Zintl Phase

Jing-Tai Zhao and John D. Corbett*

Ames Laboratory[1] and Department of Chemistry, Iowa State University, Ames, Iowa 50011

Received May 25, 1994[⊗]

The structures of the isostructural La_3In_5 and β-Y_3In_5, Pu_3Pd_5-type, have been refined and analyzed (*Cmcm*, $Z = 4$, $a = 10.345(4)$ Å, 9.840(3) Å, $b = 8.424(6)$ Å, 8.002(9) Å, $c = 10.643(6)$ Å, 10.315(5) Å, $R/R_w = 1.9/2.1$, 2.4/2.4%, respectively). A somewhat slow first-order phase transition of the latter to (α)Y_3In_5 (Tm_3Ga_5-type) occurs in the neighborhood of 900−1000 °C (*Pnma*, $Z = 4$, $a = 12.219(7)$ Å, $b = 10.328(7)$ Å, $c = 6.424(3)$ Å, $R/R_w = 5.0/5.1\%$). The former structures contain well-defined indium square pyramids (C_{2v}, d(In−In) ~ 3.0−3.2 Å) with minimum intercluster separations of 3.43 and 3.58 Å in the larger lanthanum compound, 0.2−0.3 Å less in β-Y_3In_5. Clusters in the low-temperature (α)Y_3In_5 phase have been twisted and joined by short bonds at trans-basal positions into chains that are more weakly interconnected (as above) into a three-dimensional structure. All three phases are poorly metallic (ϱ_{295} ~ 90, 47, 47 $\mu\Omega$ cm, respectively) and Pauli-paramagnetic-like, La_3In_5 having the smallest χ_M value (4×10^{-4} emu mol^{-1}). The apparent In_5^{9-} cluster in La_3In_5 can in the classical limit be readily described as a closed shell, nido-deltahedron, and the compound structurally, as a Zintl phase. The obviously important bonding that gives such clear definition of clustering makes it appropriate to refer to La_3In_5 as a "metallic Zintl phase", downplaying the delocalization of a few of the least tightly bound electrons.

Introduction

The development of new solid state materials demands more and more understanding of properties as they relate to structure. Among the empirical theories dealing with the structure−bonding−property relationships, the Zintl−Klemm concepts regarding what are often classical bonding situations (via the octet rule)[2] have been frequently applied to a broad range of main-group-element compounds in which one component is quite electropositive, usually an alkali or alkaline-earth metal.[3] However, the breadth of the applicability of these "rules" has not been widely explored, and the semiconductivities implied for the many examples have seldom been confirmed. Therefore, it is important to examine and to understand more of the structures and properties of compounds in this category. Failure of these simple guidelines in one sense occurs when such a polar compound in a seemingly suitable structure instead shows more or less traditional metallic characteristics. This may occur when the posttransition (or less electropositive main-group) component lies too far to the left, beyond the so called Zintl boundary (the silicon family or tetrels) or, presumably, when the electropositive member is more polarizing, as with one of the early transition metals. However, simple chemical understanding may be lost if these examples are dismissed too quickly. The more complex situation present in semimetallic examples does not, per se, violate the spirit of the Zintl phase classification.

The drive for closed-shell bonding of Zintl phases may manifest itself in electron-poor phases, even simple binary examples, not only through network formation ($CaSi_2$, NaTl types) but also by the appearance of "naked" clusters exhibiting more or less nonclassical (cluster-delocalized) bonding, as with the many "Zintl ions".[4] Many new hypoelectronic specimens were recently identified in alkali-metal compounds of the heavy triels In and Tl, e.g., In_{11}^{7-}[5] and Tl_9^{9-}.[6] Of particular importance in some of these, and for some of the phases described here, is the categorical conflict between the evidently strong bonding exhibited by the cluster formation and a remnant conductivity characteristic of a poor metal. In a broader sense, compounds of the aluminum family with active metals afford many ways to test the limits of 8-N rules and classical bonding concepts as well as to examine a new, rich, and diverse solid state chemistry.

The suitability of the simplest Zintl concepts in rare-earth-metal compounds of the triel elements would seem plausible for Mn_5Si_3-type R_5Ga_3 phases, in which isolated Ga^{-5} would be a necessary oxidation state. However, this assignment has been found lacking since these phases show metallic characteristics,[7] but the applicability of the ideas to the analogous indium phases R_5In_3 may be possible.[8] The question of the utility of Zintl−Klemm ideas with the In- (or Ga-) richer compounds R_3Tr_5 (Tr = triel) is the major objective of this investigation. Clusters or networks of indium (thallium or gallium) are present in the structure types of numerous compounds reported with this composition, though these particular bonding features have not been described in the literature, and no confirmatory property measurements have been included. In particular, the structures of both La_3In_5[9-11] and Y_3In_5[10,11] (along with many other R_3In_5 and R_3Tl_5 examples) have been tentatively assigned as Pu_3Pd_5 types, but only on the basis of powder diffraction data. The original report of the Pu_3Pd_5 structure made no note of the presence of a well-bonded fragment of the more electronegative element (Pd), the analysis

⊗ Abstract published in *Advance ACS Abstracts,* December 15, 1994.
(1) Ames Laboratory is operated for the U.S. Department of Energy by Iowa State University under Contract No. W-7405-Eng-82. This research was supported by the Office of the Basic Energy Sciences, Materials Sciences Division, DOE.
(2) (a) Zintl, E. *Angew. Chem.* **1939**, *52*, 1. (b) Klemm, W.; Busmann, E. *Z. Anorg. Allg. Chem.* **1963**, *319*, 297.
(3) Schäfer, H. *Annu. Rev. Mater. Sci.* **1985**, *15*, 1.
(4) Corbett, J. D. *Chem. Rev.* **1985**, *85*, 383.
(5) Sevov, S. C.; Corbett, J. D. *Inorg. Chem.* **1991**, *30*, 4875.
(6) Dong, Z.-C.; Corbett, J. D. *J. Am. Chem. Soc.* **1994**, *116*, 3429.
(7) Zhao, J.-T.; Corbett, J. D. *J. Alloys Compd.* **1994**, *210*, 1.
(8) Zhao, J.-T.; Corbett, J. D. Unpublished research.
(9) McMasters, O. D.; Gschneidner, K. A., Jr. *J. Less-Common Met.* **1974**, *38*, 137.
(10) Delfino, D.; Saccone, A.; Mazzone, D.; Ferro, R. *J. Less-Common Met.* **1981**, *81*, 45.
(11) Yatsenko, S. P.; Semyannikov, A. A.; Shakarov, H. O.; Fedorova, E. G. *J. Less-Common Met.* **1983**, *90*, 95.

0020-1669/95/1334-0378$09.00/0

Table 1. Synthetic Results and Cell Parameters (Å, Å^3) for Orthorhombic R_3In_5 Phases[a]

compn	synth cond[b]	product type (%)[c]	*a*	*b*	*c*	*V*
$La_3In_{4.5}$	1	P (80)	10.349(4)	8.401(3)	10.644(4)	925.5(6)
$La_3In_{4.75}$	1	P (85[d])	10.346(6)	8.408(4)	10.643(7)	925.8(9)
La_3In_5	1	P (90[d])	10.349(4)	8.399(3)	10.643(5)	925.1(6)
La_3In_5[e]	2	P (90[d])	10.345(4)	8.424(6)	10.643(6)	927(2)
$La_3In_{5.25}$	1	P (70)	10.343(2)	8.401(2)	10.640(2)	924.6(3)
Y_3In_5[e]	2	P(β)(100)	9.840(3)	8.002(9)	10.315(5)	812(2)
Y_3In_5[e]	3	T(α) (100)	12.219(7)	10.328(7)	6.424(3)	811(1)
$Y_3In_{4.5}$	1	T (>90)	12.237(2)	10.343(1)	6.4156(8)	812.0(2)
Y_3In_6	1	T (40)	12.252(7)	10.338(3)	6.415(4)	812.5(8)

[a] Guinier data with Si as internal standard, 22 °C, λ = 1.540 562 Å. [b] T = tube furnace; I = induction heating, $\leq 5 \times 10^{-6}$ Torr; H = high-temperature vacuum furnace; Q = quench. (**1**) H: 500 °C, 4 h (at temperature); 800 °C, 12 h; to 1250 °C slowly, 0.5 h; to RT over 6 h. Then T: 850 °C, 80 h. (**2**) T: 350 °C, 12 h; 400 °C, 40 h; 30 °C/h to 1180 °C, 12 h; 5 °C/h to 1100 °C, 0.5 h; 20 °C/h to 1000 °C, 170 h. Then Q. (**3**) I: 400 °C, 20 h; 1400 °C, 2 h; 1000 °C, 1 h; 700 °C, 24 h. [c] P: Pu_3Pd_5 type, *Cmcm*. T: Tm_3Ga_5 (low-temperature) type, *Pnma*. [d] See text in Experimental Section regarding $LaIn_2$ impurity content. [e] Sources of crystals for structural studies.

pertaining only to geometrics of neighboring atom polyhedra with quite wide distance distributions.[12] The corresponding R_3Ga_5 compounds with smaller R = Sc, Y, Tb–Tm, Lu have been described in terms of the new Tm_3Ga_5 structure type,[13] but again the description of the last dealt largely with the polyhedral aspects of the structure, not the Ga–Ga bonding. No R_3In_5 examples of this type have been reported. Uncertainties regarding the structures, properties, and bonding of these indium compounds have led us to investigate them further.

Experimental Section

Synthesis. The rare-earth metals used in the syntheses were Ames Laboratory products while the In, 6–9's purity, was from Johnson-Matthey. The R_3In_5 samples were all prepared by direct reaction of the pure components in welded Ta containers within tube furnaces or by induction heating. The sample loadings were all done in a He-filled glovebox. The rare-earth-metal rods or sheets were scraped clean with a scalpel before the cutting and weighing. The pure components were loaded in a Ta tube already welded at one end, and the other end was then tightly crimped before welding under He. For tube furnace reactions, the Ta containers were enclosed in fused silica jackets, and these were flame-baked under a good vacuum ($\sim 10^{-5}$ Torr) before sealing. The reaction conditions and estimated yields (based on powder pattern intensities) are listed in Table 1; these generally entailed heating to 1200–1400 °C followed by extended annealing at 750–1000 °C. The persistence of $LaIn_2$ in substantially all samples near the La_3In_5 composition suggested that its melting relationships may differ from the simple congruency concluded before.[9] One explanation, analogous to that established for Zr_5Sn_3–Zr_5Sn_4,[14] is that the maximum melting point of the evidently nonstoichiometric La_3In_5 may logically lie on the indium-rich side, closer to the high melting $LaIn_2$. If so, slow cooling can then give a sample that is physically segregated on a macroscopic scale and accordingly does not readily anneal to the equilibrium phase content. This hypothesis seemed reasonable as a pressed pellet of a ground product, which process reduces the scale of the composition separations, was found to go from roughly 20% to 10% $LaIn_2$ after only 2 days at 870 °C.

X-ray Characterization. Powder diffraction data obtained with the aid of an Enraf-Nonius Guinier camera and Cu Kα_1 radiation were used for phase identification. The films were compared with the patterns calculated for phases with known structures. The cell parameters listed in Table 1 were obtained by least-squares refinements of measured 2θ values with NIST (NBS) silicon as an internal standard. The content of mixtures was estimated visually on the basis of powder pattern intensities and, if appropriate, unit cell contents as well.

Single crystals of La_3In_5 and of α- (low temperature) and β-Y_3In_5 for diffraction studies were selected from crushed bulk samples, mounted in thin-walled glass capillaries inside a N_2-filled glovebox, and checked by either Laue or oscillation photographs prior to data collection. Diffraction data were collected at room temperature on either Rigaku AFC6R or Enraf-Nonius CAD4 four-circle automatic diffractometers with monochromated Mo Kα radiation. Systematic extinctions led to the assignment of the space groups, and these were confirmed by the structural refinements, which were carried out by using program package TEXSAN.[15] The significant absorption corrections were in each case accomplished empirically, first, according to the average of ψ-scan curves for three strong reflections with different θ values and, subsequently, by DIFABS, as recommended when there is substantial absorption.[16] Anomalous dispersion by the elements was taken into account during the refinements. The refinements and results for La_3In_5 and β-Y_3In_5 were entirely routine and normal. On the other hand, the α-Y_3In_5 result exhibited small, fairly uniform ellipsoids but higher *R* values and residual electron densities in a ΔF map up to 5.8 e/Å^3. The last made no sense chemically. The differences are thought to arise from a reduced quality of the crystal obtained via the sluggish first-order transition that occurs (see Results) when β-Y_3In_5 is annealed at 700 °C for 24 h. The other data crystals came from melt cooling and annealing at significantly higher temperatures (Table 1).

Table 2. Selected Details of Structural Refinements of R_3In_5 Compounds

	La_3In_5	α-Y_3In_5	β-Y_3In_5
space group, Z	*Cmcm* (No. 63), 4	*Pnma* (No. 62), 4	*Cmcm* (No. 63), 4
fw	990.83	840.82	840.82
cell params[a]			
a (Å)	10.345(4)	12.219(7)	9.840(3)
b (Å)	8.424(6)	10.328(7)	8.002(9)
c (Å)	10.643(6)	6.424(3)	10.315(5)
d_{calc}, g cm^{-3}	7.10	6.89	6.88
μ(Mo Kα) (cm^{-1})	255.05	351.17	349.53
transm coeff range	0.79–1.07	0.85–1.17	0.88–1.13
R^b/R_w^c (%)	1.9/2.1	5.1/5.0	2.4/2.4

[a] Guinier data; see Table 1 for sources. [b] $R = \sum||F_o| - |F_c||/\sum|F_o|$. [c] $R_w = [\sum w(|F_o| - |F_c|)^2/\sum w(F_o)^2]^{1/2}$, $w = \sigma_F^{-2}$.

Selected details regarding the three data collections and refinements are listed in Table 2. The atomic positional and isotropic-equivalent thermal parameters are listed in Table 3 with the atoms assigned as in the original reports. More details on the structural studies as well as the anisotropic displacement parameters are given in the supplementary material; these as well as the structure factor data are also available from J.D.C.

Property Measurements. Resistivities of La_3In_5 and of α- and β-Y_3In_5 samples with average grain sizes of ~ 200 μm that had been diluted with chromatographic alumina were measured at 34 or 36 MHz by the Q method,[17] which is based on the change of the quality factor caused by microwave skin absorption in suitably sized grains of the samples. The new apparatus utilizes a Hewlett-Packard 4342A Q meter, cooling controls, and improved shielding and operates between ~90 and 290

(12) Cromer, D. T. *Acta Crystallogr.* **1976**, *B22*, 1930.
(13) Yatsenko, S. P.; Hladyshewsky, E. I.; Tschuntonow, K. A.; Yarmolyuk, Ya, P.; Hryń, Yu. N. *J. Less-Common Met.* **1983**, *91*, 21.
(14) Kwon, Y.-U.; Corbett, J. D. *Chem. Mater.* **1990**, *2*, 27.
(15) *TEXSAN*, version 6.0 package; Molecular Structure Corp.: The Woodlands, TX, 1990.
(16) Walker, N.; Stuart, D. *Acta Crystallogr.* **1983**, *A39*, 158.
(17) Shinar, J.; Dehner, B.; Beaudry, B. J.; Peterson, D. T. *Phys. Rev.* **1988**, *B37*, 2066.

Table 3. Positional and Isotropic Displacement Parameters for R_3In_5 Phases

atom	position	x	y	z	B_{iso},[a] (Å^2)
			La_3In_5		
La1	4*c*	0	0.63279(7)	1/4	0.91(2)
La2	8*e*	0.20413(3)	0	0	0.84(2)
In1	4*c*	0	0.01599(9)	1/4	1.14(3)
In2	8*f*	0	0.30783(7)	0.44708(5)	1.03(2)
In3	8*g*	0.20863(4)	0.28792(7)	1/4	1.12(2)
			β-Y_3In_5		
Y1		0	0.6228(2)	1/4	0.71(8)
Y2		0.2044(1)	0	0	0.71(6)
In1		0	0.0076(2)	1/4	0.77(6)
In2		0	0.3078(1)	0.4539(1)	0.70(4)
In3		0.2164(1)	0.2902(1)	1/4	0.83(4)
			α-Y_3In_5		
Y1	4*c*	0.0598(2)	1/4	0.6494(2)	0.38(8)
Y2	8*d*	0.1441(1)	0.0057(2)	0.1095(2)	0.38(5)
In1	4*c*	0.5048(2)	1/4	0.3835(3)	0.59(6)
In2	4*c*	0.2476(2)	1/4	0.3470(3)	0.54(6)
In3	4*c*	0.2860(2)	1/4	0.8745(3)	0.58(6)
In4	8*d*	0.4020(1)	0.0460(1)	0.1235(2)	0.44(4)

[a] $B_{iso} = (8\pi^2/3)\sum_i\sum_j U_{ij}a_i^*a_j^*\vec{a}_i\vec{a}_j$.

K. The resistivity values have been generally found to be correct within a factor of 3, while the temperature coefficients should be quite reliable. Samples sealed under He for magnetic susceptibility measurements were held between two fused silica rods that were in turn fixed inside a silica tube.[18] The measurements were carried out over 6−300 K on a Quantum Design (MPMS) SQUID magnetometer, and the data were corrected for the container and the standard diamagnetic core contributions.

Results and Discussion

Structures. On the basis of the behavior of other alkali- and alkaline-earth-metal compounds of both gallium and indium, one would expect In−In or Ga−Ga bonds in structures with R_3In_5 or R_3Ga_5 compositions since these compounds are electron deficient with respect to the probable (ideal) closed-shell states for isolated atoms, that is, the −5 oxidation states In^{-5} or Ga^{-5}. Of course, the more polarizing R^{3+} cations in these compounds make such predictions and explanations more problematic with respect to simple Zintl concepts. As expected, the structures of all of these compounds show considerable In−In or Ga−Ga bonding, sometimes in more networklike arrays, but to some degree approaching the ideal clustering predicted by Wade's rules.

Figure 1 shows the cation positions and the indium atom connectivities in La_3In_5 in a Pu_3Pd_5-type structure; the same general view pertains to β- (high-temperature) Y_3In_5. One can easily recognize well-defined square (C_{2v}) pyramids of indium with distances in the range 3.01−3.23 Å (heavy lines). These are more distantly interconnected (light lines) to form a network structure. Sheets of similarly oriented clusters in weakly bound 8-nets alternate along [001], as shown in Figure 2 (normal to Figure 1), while a weak 10-net can also be discerned along [001], Figure 1. There is little to distinguish the quality attained for the structures of La_3In_5 and β-Y_3In_5 except that the yttrium example experimentally refined with slightly larger errors but smaller ellipsoids. Mean In−In distances within the pyramids in both are similar, 3.10(4) Å (La_3In_5) and 3.07(3) Å (β-Y_3In_5) (where the errors reflect the range). The In−In distances are shortest within the pyramidal base (~3.01 Å) where the atoms are formally three-bonded. (The Pauling single-bond metallic

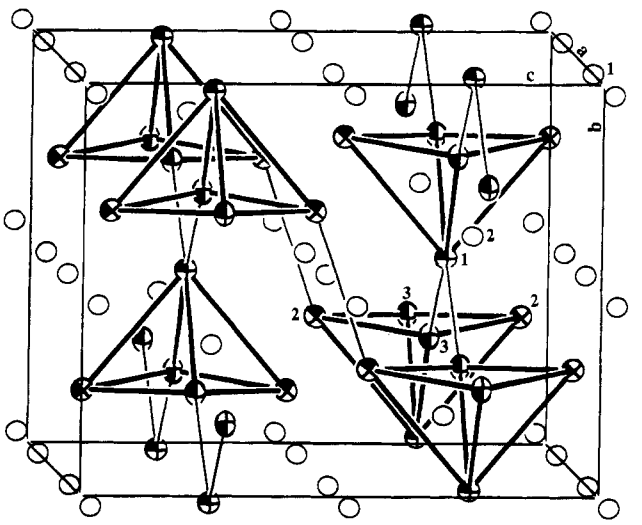

Figure 1. [100] view of the orthorhombic structure of La_3In_5 (Pu_3Pd_5-type) with the In_5 clusters emphasized (d(In−In) = 3.01−3.23 Å). The lighter intercluster lines represent separations of 3.43 Å (at In2) and 3.58 Å (In1).

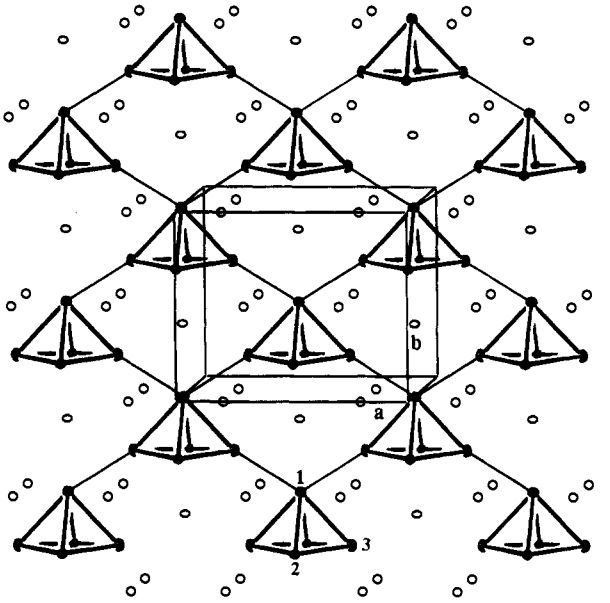

Figure 2. [001] view of the vertical layers of clusters at z = 1/4, 3/4 in La_3In_5, Figure 1.

distance is ~2.96 Å,[19] and 2.91−3.02 Å is common in normal single bonds between clusters in many indium network structures.[20])

The indium square pyramids in La_3In_5 are weakly interbonded (light lines) at distances of 3.428(3) Å (×2) (In2−In3) and 3.575(2) Å (×2) (In1−In3) vs the distinctly shorter separations, 3.220(4) and 3.289(2) Å, respectively, in β-Y_3In_5 (Table 4), in each instance with the greater distance at the vertex (In1). The intercluster distances in La_3In_5 correspond to respective Pauling bond orders of only 0.17 and 0.10 vs 0.38 and 0.29 in Y_3In_5. The appreciable differences in these intercluster distances between La_3In_5 and Y_3In_5 can be best understood in terms of a simple matrix effect, that is, separations that are largely dictated

(18) Sevov, S. C.; Corbett, J. D. *Inorg. Chem.* **1992**, *31*, 1895.

(19) Pearson, W. B. *The Crystal Chemistry and Physics of Metals and Alloys*; Wiley-Interscience; New York, 1972; p 151. This contains R_{12} data that update the original values (D_1(In) = 2.942 Å): Pauling, L. *The Nature of the Chemical Bond*; Cornell University Press: Ithaca, NY, 1960; p 400.

(20) Sevov, S. C.; Corbett, J. D. *Inorg. Chem.* **1993**, *32*, 1612 and references therein.

Table 4. Interatomic Distances (Å) in La_3In_5 and β-Y_3In_5 (Pu_3Pd_5-Type)

	La_3In_5	β-Y_3In_5		La_3In_5	β-Y_3In_5
R1−4R2	4.207(1)	4.010(2)	R1−2In2	3.449(2)	3.283(3)
R1−In1	3.228(3)	3.079(4)	R1−2In3	3.285(1)	3.096(2)
R1−2In2	3.263(2)	3.104(2)	R1−2In3	3.619(2)	3.409(3)
R2−2R1	4.207(1)	4.010(2)	R2−2In2	3.391(2)	3.215(3)
R2−R2	4.224(2)	4.022(3)	R2−2In2	3.508(1)	3.325(2)
R2−2R2	4.317(3)	4.101(4)	R2−2In3	3.330(1)	3.174(2)
R2−2In1	3.400(1)	3.271(1)	R2−2In3	3.601(2)	3.472(2)
In1−R1	3.228(3)	3.079(4)	In1−2In3	3.147(2)	3.106(2)
In1−4R2	3.400(1)	3.271(1)	In1−2In3[a]	3.575(2)	3.289(2)
In1−2In2	3.232(2)	3.193(3)			
In2−R1	3.263(2)	3.104(2)	In2−In1	3.232(2)	3.193(3)
In2−R1	3.449(2)	3.283(3)	In2−In2[a]	3.428(3)	3.220(4)
In2−2R2	3.391(2)	3.215(3)	In2−2In3	3.014(1)	2.996(1)
In2−2R2	3.508(1)	3.325(2)			
In3−R1	3.285(1)	3.096(2)	In3−In1	3.147(2)	3.106(2)
In3−2R2	3.330(1)	3.174(2)	In3−In1	3.575(1)	3.289(2)
In3−2R2	3.601(2)	3.472(2)	In3−2In2	3.014(1)	2.996(1)

[a] Interpyramidal distances.

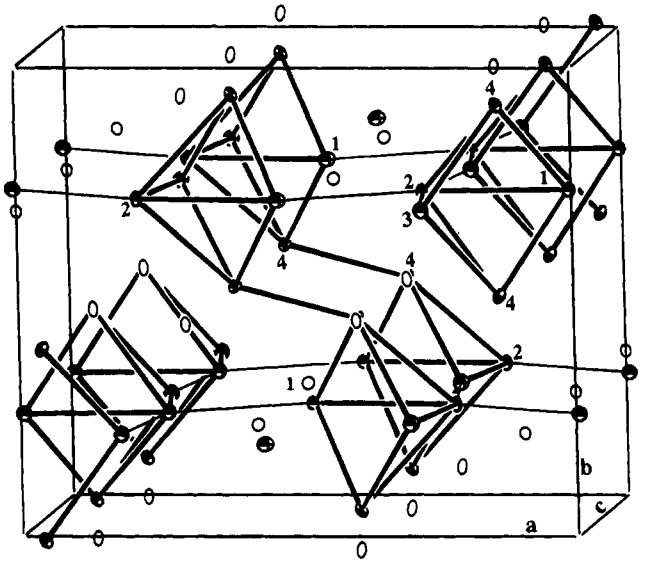

Figure 3. [001] view of the structure of α-Y_3In_5 (Tm_3Ga_5-type) with In−In separations of 2.97−3.17 Å represented by heavy lines. The short intercluster (In4−In4) separations of 3.03 Å generate vertical zigzag chains of clusters. The lighter lines represent longer intercluster distances of 3.32−3.42 Å.

by relative cation sizes. This is important because, in the ideal limit of no intercluster bonding, the phases are valence compounds with square pyramidal *nido*-In_5^{9-} units containing $2n + 4$ skeletal (p) electrons above the s cores (see below). Although it is hard to say how strong these intercluster bonds are, it appears that they are still significant enough (in the resulting bands) to change the properties of both compounds from semiconducting to metallic (below).

Figure 3 shows the related structure of α-Y_3In_5 (Tm_3Ga_5 type[13]), a new polytype for this compound and the first indide example, that was achieved on annealing the β-phase for 24 h either at 700 °C in high vacuum or at 850 °C in a sealed container. (The former eliminates hydrogen as a possible factor in the stability.[21]) The gross features of the prototype structure, which have not been described before, are similar to those of the high-temperature phase in that it consists of interlinked indium square pyramids. The major difference between the two

(21) Leon-Escamilla, E. A.; Corbett, J. D. *J. Alloys Compd.* **1994**, *206*, L15.

Table 5. Interatomic Distances (Å) in α-Y_3In_5 (Tm_3Ga_5-Type)[a]

Y1−2Y2	3.870(3)	In2−In1	3.153(3)
Y1−In1	3.075(3)	In2−In1[b]	3.315(3)
Y1−In2	3.006(3)	In2−In3	3.072(3)
Y1−In3	3.118(3)	In2−In3[b]	3.421(3)
Y1−In3	3.350(4)	In2−2In4	3.172(2)
Y1−2In4	3.097(3)	In2−Y1	3.006(3)
Y1−2In4	3.352(3)	In2−2Y2	3.302(3)
		In2−2Y2	3.311(3)
Y2−Y1	3.870(3)		
Y2−Y2	3.794(4)	In3−In2	3.072(3)
Y2−In1	3.142(3)	In3−In2[b]	3.421(3)
Y2−In2	3.302(3)	In3−2In4	3.001(2)
Y2−In2	3.311(3)	In3−Y1	3.118(3)
Y2−In3	3.162(3)	In3−Y1	3.350(4)
Y2−In4	3.197(3)	In3−2Y2	3.162(3)
Y2−In4	3.200(2)		
Y2−In4	3.375(3)	In4−In1	2.968(2)
		In4−In2	3.172(2)
		In4−In3	3.001(2)
In1−In2	3.153(3)	In4−In4	3.026(3)
In1−In2[b]	3.315(3)	In4−Y1	3.097(3)
In1−2In4	2.968(2)	In4−Y1	3.352(3)
In1−Y1	3.075(3)	In4−Y2	3.197(3)
In1−2Y2	3.142(3)	In4−Y2	3.200(2)
In4−Y2	3.375(3)		

[a] Distances for Y−Y < 4.0 Å, Y−In < 3.4 Å. [b] Inter-In_5 distances.

is the connectivities, as shown in Figure 3 for two cell contents along [001]. The clusters in the high-temperature phase have been reoriented into a lower symmetry arrangement with slightly higher density. The "square" pyramids now lie on mirror planes at $y = 1/4, 3/4$ with In2 as apices. They still exhibit similar internal dimensions that average 3.06(3) Å overall, with the shorter members ($\bar{d} = 2.98(1)$ Å) again in the base (Table 5). A major change appears in the In4−In4 separations between opposite corners of pyramidal bases in adjoining clusters (vs In2−In2 in β-Y_3In_5, Figure 1) which are now relatively short, 3.026 (3) Å (bond order 0.79), and marked with heavier lines in Figure 3. This generates zigzag chains of strongly linked clusters along $\vec{b}$, vertical in Figure 3, which correspond to linkage along $\vec{c}$ in the high-temperature form but after considerable cluster rotation and twisting. The (010) layers normal to this view, Figure 4, illustrate the weakly bound 8-net via interconnections of apices (In2) to opposite basal corners (In1 and In3) and vice versa. Layers of this type with opposite orientations are interconnected by the short intercluster In4−In4 bonds seen in Figure 3. The twisting of the clusters in the low-temperature form and the change of bond angles between them are quite obvious on comparison of Figures 2 and 4, and the weak linkages are very similar in length in both. The electronics of this relaxation would be worth an exploration. Presumably many of the corresponding isostructural R_3Ga_5 (R = Sc, Y, Tb−Tm, Lu) have similar structural features, transitions, and physical properties.

Phase Transition. The low-temperature (Tm_3Ga_5-type) structure for α-Y_3In_5 is a new polymorph for any Pu_3Pd_5-type phase, only the gallides of the smaller rare-earth-metals previously being reported with the Tm_3Ga_5 structure. Single α-phase samples were obtained after annealing at either 850 or 700 °C for 24 h, but we saw no sign of this form for La_3In_5 (Table 1). Annealing of unspecified Pu_3Pd_5-type rare-earth-metal indides at 900 °C for 3 days[7] or below the peritectic temperatures[8] have apparently not produced this change. The transformation may have been missed in DTA studies since the transition is fairly sluggish and could not be accomplished during slow cooling but only through annealing. The transition must be first order since the two structures are not symmetry related. There are also hints, but few specifics, about possible high-temperature

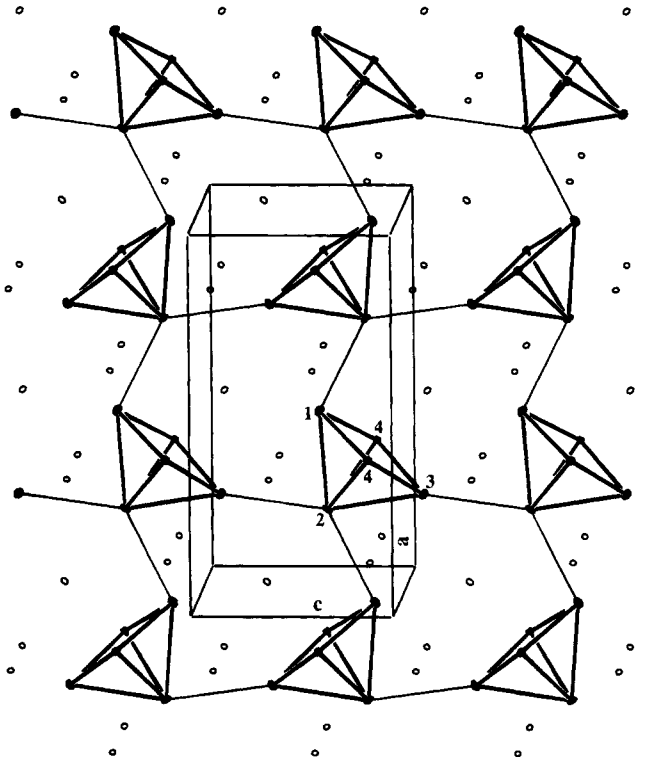

Figure 4. [010] view of the longer links between clusters in α-Y_3In_5, the 8-net formed, and the cluster rotations (compare Figure 2).

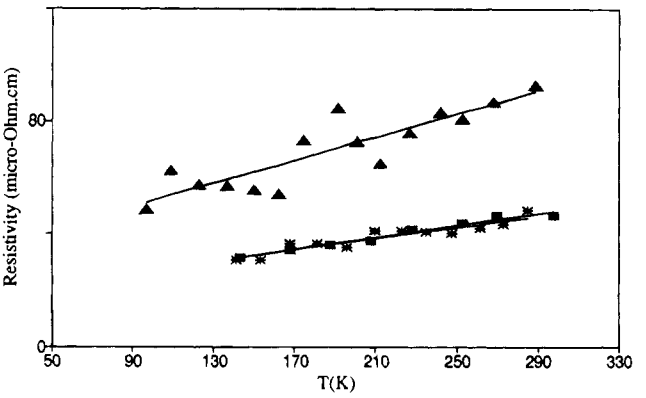

Figure 5. Resistivities (μΩ cm) vs temperature (K): ▲, La_3In_5; *, β-Y_3In_5; ■, α-Y_3In_5.

transitions that were seen in DTA analyses of some of these Pu_3Pd_5 structures,[10,22] but it is not clear that these have any relevance to the present work.

Properties. Resistivities (Q method) and magnetic susceptibilities were measured for all three of the phases reported here, Figures 5 and 6. The La_3In_5 data pertain to a sample that also contained 10% $LaIn_2$ (see Synthesis), which has a $CeCu_2$-(distorted-AlB_2-) type structure and is probably metallic. The contactless method is based on RF skin absorption, so the responses should be proportional in the RF absorption volume of the individual grains (~200 μm). Thus the meaning of the results is only slightly clouded. The compound appears to be poorly metallic ($\varrho_{295} \sim 90$ μΩ cm) and Pauli-paramagnetic ($\chi_M \sim 4 \times 10^{-4}$ emu mol^{-1}). Both forms of Y_3In_5 are moderately poor conductors, with $\varrho_{295} \sim 47$ μΩ cm for each and metallic in their temperature dependencies. The magnetic susceptibility of the low-temperature (Tm_3Ga_5-type) Y_3In_5 phase is distinctly more positive than that of La_3In_5 and varies only slightly with

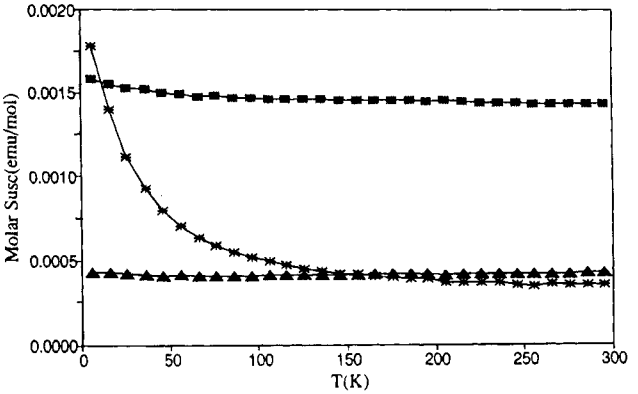

Figure 6. Molar magnetic susceptibilities as a function of temperature: ▲, La_3In_5; *, β-Y_3In_5; ■, α-Y_3In_5.

temperature, which may indicate that the electrons on the Fermi surface have some d character.[23] On the other hand, the susceptibility of (metastable) β-Y_3In_5 is temperature dependent, particularly below ~150 K, Figure 6, and very different from that of α-Y_3In_5. A transition at low temperatures may be involved, but the behavior is not understood.

Bonding. The three R_3In_5 structures described here contain a novel and persistent feature, square pyramidal In_5 clusters as building blocks. The structure of low temperature (α)Y_3In_5 reasonably reflects a greater number of In−In bonds that are, on average, somewhat shorter, and the square pyramids, though recognizable, are difficult to single out for their bonding significance because of the short In4−In4 interconnections. Furthermore, differences between the isotypic La_3In_5 and β-Y_3In_5 are also striking. The substantial 0.29 and 0.21 Å decreases between La and Y in intercluster separations (Figure 1) at the pyramidal vertices (In1) and opposite corners of the square base (In2), respectively, appear to follow by some scaling factor the reduction in ideal cation sizes (0.14 Å[24]) and in R−In distances (0.13−0.21 Å). The long 3.43 and 3.58 Å intercluster separations in La_3In_5 are particularly interesting as they seem to be more nearly incidental from a structural and, we can imagine, an electronic point of view.

The foregoing seem important since the bonding in an isolated square pyramid constructed of main-group elements is well described by Wade−Mingos rules[25] —a nido cluster bonded by $2n + 4$ skeletal electrons, 14 in this case, above one more-or-less s pair (≃nonbonding core) orbital from each indium. This corresponds exactly to In_5^{9-}, suggesting that the composition La_3In_5 could be closed shell and a Zintl phase. This precise limit is unlikely for the present compound, but it is still a very useful reference for categorizing the structure and bonding. Several circumstances possibly come into involvement regarding the conductivity. First and foremost, the four interactions that each cluster has with its neighbors, the pairs of distances corresponding to bond orders of about 0.17 and 0.09 each, probably cannot be neglected. These should broaden the higher lying cluster orbitals, perhaps sufficiently to overlap the neighboring empty cluster states indirectly or directly. Covalency between La and In clusters will function similarly, particularly with the higher field of La^{3+}. (Compare the mixing in $Ba_5Ga_6H_2$.[26]) In fact, one should be concerned whether the polarity difference between La and In is sufficient in any case to keep a gap open since the negative charge formally ac-

(22) Delfino, S.; Saccone, A.; Ferro, R. *Z. Metallk.* **1983**, *74*, 674.
(23) Martin, D. H. *Magnetism in Solids*, The MIT Press: Cambridge, MA, 1967; p 215.
(24) Shannon, R. P. *Acta Crystallogr.* **1976**, *A32*, 751.
(25) (a) Wade, K. *Adv. Inorg. Radiochem.* **1976**, *18*, 1. (b) Mingos, D. M. P. *Acc. Chem. Res.* **1984**, *17*, 311.

cumulated on In will of course raise its valence (H_{ii}) energies and reduce the difference between the two elements. Calculations assisting our vision on these points are clearly called for and are in progress together with studies on isomorphous phases with different electron counts (e.g., Ba_3Pb_5, La_3Sn_5).[27]

Notwithstanding, we should not lose sight of the clearly important In−In bonding that gives, and persists in, this novel structure. The intracluster distances are obviously characteristic of strong bonding, for which we fortunately have many recent examples of what is important and possible in formal anionic arrays.[5,18,20,28] Lower lying, more-or-less localized, states contribute to the bonding reflected by the In_5 clustering, irrespective what is happening at the highest (Fermi) level where some delocalization of screened electrons is also present, albeit it relatively slight. The term "metallic Zintl phase" seems very appropriate in such situations to recognize what appears to be most important in the structure. It would be a great mistake to ignore this and use only the weak metal-like conduction for classification. Nesper[29,30] has discussed similar circumstances.

It is very likely that many more examples of this type are to be found among so-called Zintl phases. Hughbanks[31] has reminded us that a very common criterion for a Zintl phase (valence compound) classification is that the *structure* looks like it ought to qualify. The fraction of such phases for which the presumed semiconduction has been verified is small indeed. Furthermore, we find many other examples among the alkali-metal−indium or −thallium systems in which calculations or long established Wade's rules predict that anionic clusters like $In_{10}Hg^{8-}$,[32] $In_{10}Zn^{8-}$,[33] Tl_{13}^{10-},[34] and In_4^{8-}[35] should exhibit closed-shell configurations, yet these phases are in fact poor metals in the solid state ($\varrho_{295} \sim 50-600\ \mu\Omega$ cm). A great deal of insight would be lost if the electronics of the clustering and bonding were to be ignored and great importance attached instead to a small number of electron carriers. Relatively high charges are necessary in many clusters of elements like In and Tl for which electron affinities must be quite small. The much more surprising feature is that so much clustering is found for these at all.

None of the other compounds of neighboring elements that have been reported to have the Pu_3Pd_5 structure would appear to afford as clear a picture of this bonding property. The remaining lanthanide members R_3In_5, R = Ce−Er,[36] are all smaller and are expected to have shorter intercluster interactions, as with yttrium. A similar change is expected for La_3Tl_5. Both Ba_3Pb_5 (which is not a hydride[37]) and R_3Sn_5, R = La−Pr, are electron-rich (for Sn_5^{4-} etc.) and are presumably better metals. No gallium analogues are known except with uranium and zirconium. The fact that no examples are known that are electron-poorer than La_3In_5 is, of course, indirectly supportive of the gross features of the Zintl phase assignment as well. Finally, Pu_3Pd_5 itself[12] is not a very useful example, at least at this time. As with $Pu_{31}Pt_{20}$ vs $Ca_{31}Sn_{20}$,[38] there are no clear ideas as to what bonding levels constitute a closed-shell configuration for a cluster of the late, heavy transition metals or what is an appropriate oxidation state for plutonium cations. Furthermore, the clusters are not nearly as well isolated; the intercluster Pd2−Pd2 distance (2.82(1) Å, Pauling bond order 0.38) is as short as the average within in the Pd_5 cluster, while the other bridging separation Pd1−Pd3 (3.08 Å) is longer and comparable to that found here. Changes seen in the electron-rich La_3Sn_5 are in part similar.[27]

We expect it will only be a short while before more isolated In_5^{9-} ions (or one of its analogues) are discovered in other systems as well, probably with a greater proportion of lower-charged cations. The stability of such cluster species in solid compounds appears to be very sensitive to packing. Alkali-metal cations in many indium or thallium cluster or network compounds exhibit quite specific interactions about cluster vertices, edges, and faces, and we have repeatedly found that new species can be isolated in solid phases simply by changing or, especially, mixing the cations with respect to size or, presumably, charge.[6,20,34]

Acknowledgment. The authors are indebted to H. F. Franzen for the use of arc-melting and induction furnaces and to J. Ostenson and D. Finnemore for the magnetic data.

Supplementary Material Available: A listing of further data collection and refinement information and a table of anisotropic displacement parameters for all of the structures reported (3 pages). Ordering information is given on any current masthead page.

IC940586O

(26) Liu, Q.; Hoffmann, R.; Corbett, J. D. *J. Phys. Chem.* **1994**, *98*, 9360.
(27) Harp, J.; Vaughey, J. T.; Corbett, J. D. Unpublished research, 1994.
(28) Sevov, S. C.; Corbett, J. D. *Science* **1993**, *262*, 880.
(29) Nesper, R. *Prog. Solid State Chem.* **1990**, *20*, 1.
(30) Nesper, R. *Angew. Chem., Int. Ed. Eng.* **1991**, *30*, 789.
(31) Hughbanks, T. In *Inorganometallic Chemistry*; Fehlner, T., Ed.; Plenum Press: New York; 1992; p 291.
(32) Sevov, S. C.; Corbett, J. D. *J. Alloys Compd.* **1993**, *202*, 289.
(33) Sevov, S. C.; Corbett, J. D. *Inorg. Chem.* **1993**, *32*, 1059.
(34) Dong, Z.-C.; Corbett, J. D. Unpublished research.
(35) Sevøv, S. C.; Corbett, J. D. *J. Solid State Chem.* **1993**, *103*, 114.
(36) Villars, P.; Calvert, L. D. *Pearson's Handbook of Crystallographic Data for Intermetallic Phases*, 2nd ed.; American Society for Metals International: Metals Park, OH, 1991; p 281.
(37) Leon-Escamilla, E. A. Unpublished research, 1994.
(38) Ganguli, A. K.; Guloy, A. M.; Leon-Escamilla, E. A.; Corbett, J. D. *Inorg. Chem.* **1993**, *32*, 4349.